CrystEngComm

Cite this: *CrystEngComm*, 2011, **13**, 1899

www.rsc.org/crystengcomm

PAPER

Structures and conformational analysis of a 3 × 3 isomer grid of nine *N*-(fluorophenyl)pyridinecarboxamides†

Pavle Mocilac,[a] Alan J. Lough[b] and John F. Gallagher*[a]

Received 22nd June 2010, Accepted 18th November 2010
DOI: 10.1039/c0ce00326c

A 3 × 3 isomer grid of *N*-(fluorophenyl)pyridinecarboxamides is reported and integrating crystal structure analyses, *ab initio* optimisation calculations (*gas phase* and solvated forms in CH_2Cl_2, H_2O) and conformational analyses. The nine **NxxF** isomers (x = 4-, 3- or 2-substitution on **N** and **F**) are investigated and compared to determine and correlate factors underpinning (a) the roles of the **F**/**N** atom substituents on molecular conformation and overall supramolecular aggregation, (b) competition between intermolecular amide···amide (in **NppF**) or intra-/intermolecular amide···pyridine hydrogen bond formation and (c) structural and physico-chemical properties. Crystal structure analyses of the **NxxF** isomers reveal different primary aggregation processes as either N–H···N or N–H···O=C and with **NmpF** forming an unusual cyclic N–H···N hydrogen bonded tetrameric assembly [as a $R^4_4(24)$ ring]. Compounds **NpmF** and **NpoF** are isomorphous and the latter is also disordered. Conformational analysis of the **NxxF** molecular structures from DFT calculations differs from the crystal structure results for several isomers and highlighting the co-operative effects of intra-/intermolecular interactions in the solid state.

1 Introduction

Cheminformatics has emerged in the past decade as a scientific field that is proving to be of enormous benefit for our use as scientists in analyzing a wide range of scientific problems.[1,2] One such challenge is the on-going demand to synthesise, analyse and collate vast numbers of chemical compounds and data. This information feeds directly into a global '*drug-pharma*' enterprise persistently searching for new and more effective molecules to treat a variety of newly discovered and existing maladies.[3,4] Comprehensive chemical and computational analyses of small '*drug-like*' molecules together with structural systematic approaches allow us to utilise an increasing data stream from both crystallography and computational resources.[5–8] Integration can yield essential information for analysing trends and provides an insight into similar/different physical or chemical properties, within or between molecular organic series.[5,6,8–10]

Isomer grids provide a basis for comprehensive studies incorporating (a) synthesis and characterisation, (b) *ab initio* computational and conformational analyses and (c) crystal structure analyses.[11,12] The relative energies of different molecular conformations can be compared to aid us in a detailed understanding of factors that facilitate the crystallisation and isolation of particular conformations in the solid state; unexpected conformations from theory and the solid-state can therefore be rationalised.[5,9] This is particularly relevant for compounds where rotational barriers in solution are low enough to provide the possibility of a greater diversity of molecular conformations and/or molecular disorder observed in the solid-state. This information may also assist us in understanding why some compounds readily crystallize as polymorphs and others with some difficulty.[5,8,9] Ultimately the roles that the substituent atoms/groups play in supramolecular packing and organisation in the solid state can be appraised and understood.[8–12]

Our research focus is based on *n* × *m* isomer grids of benzamides (*i.e.* fluoro- and methyl-*N*-(pyridyl)benzamides) which provide a semi-rigid, invariant scaffold to analyse the impact of different substituent atom/group (*e.g.* CH_3 or F) site variation both on the molecular conformations and physico-chemical properties.[11,12] The influence of the aromatic group substitution patterns can also be evaluated in terms of the preferred primary hydrogen bonding (N–H···N or N–H···O=C) in the solid-state, in tandem with the influence and effect of weaker interactions on molecular aggregation.[11,12]

Related scientific studies[5] have highlighted the importance of fluorine and its role in weak interactions[11,13,14] as well as the roles of **NxxF** picolinamides in biological systems.[15–17]

Herein, the synthesis and characterisation of a 3 × 3 isomer grid of nine *N*-(fluorophenyl)pyridinecarboxamides (**NxxF**)

[a]*School of Chemical Sciences, Dublin City University, Dublin 9, Ireland. Web: http://doras.dcu.ie; E-mail: john.gallagher@dcu.ie; Fax: +353-1-7005503; Tel: +353-1-7005114*
[b]*Department of Chemistry, University of Toronto, 80 St George Street, Toronto, Ontario, Canada M5S 3H6*

† Electronic supplementary information (ESI) available: The ^{1}H, ^{13}C and ^{19}F NMR and spectroscopic data and the full listings of *ab initio* calculations for all nine **NxxF** isomers. CCDC reference numbers 722730, 722731 and 781752 to 781758. For ESI and crystallographic data in CIF or other electronic format see DOI: 10.1039/c0ce00326c

(with x = *para*-/*meta*-/*ortho*-) (Scheme 1: $C_{12}H_9FN_2O$) is reported with comprehensive crystal structure and conformational analyses (calculations using CBS-QB3//B3LYP/6-311++G) on *gas-phase* and solvated forms (PCM-SMD model). The conformational features and differences between the solid-state and model conformations, together with structural and property trends, are discussed for the **NxxF** isomer grid. The amide group is reversed between the aromatic rings in comparison with our previous benzamide series[11,12] derived from 4-aminopyridine (4-AP, an experimental drug in multiple sclerosis, spinal cord injury models[18] and used as a K_v1 channel blocker[19]). A further desire is to obtain more specific or less toxic drugs, structurally similar to benzamide derivatives of 4-AP[11,12] for exploitation as potential K^+ channel blockers.[11,18–20]

NppF has previously been used as an intermediate in the synthesis of 4-pyridinium cationic-dimer antimalarials.[15] The **NmxF** triad has been studied in an unusual synthesis of nicotinamides[21] and recently **NmoF** has been cited as a promising candidate for lead design as a selective inhibitor of LmSir2, a sirtuin protein from *Leishmania*, and therefore, a potential new drug and/or scaffold for leishmaniasis drug design.[16] In the **NoxF** series, **NopF** has been incorporated as a deprotonated ligand into a Co^{III} complex[22] (**NopF** crystal structure reported recently[23]) and **NomF** as an intermediate in the synthesis of thioamide analogues (mp 65–82 °C[24] *vs.* 77.2–78.0 °C); **NooF** has been employed as a ligand in a ruthenium complex developed as a potential cytotoxic agent.[17] Overall, modest spectroscopic data are available for several of the **NxxF** isomers from these diverse reports.[15–17,21–24]

2 Experimental section

2.1 Materials and equipment

All chemicals were purchased from Sigma Aldrich except for 2-pyridinoyl chloride (Fluorochem): TLC alumina and silica plates were purchased from Fluka. Melting points were performed using a Stuart Scientific SMP40 automated melting point apparatus. IR spectroscopy was performed on a Thermo Nicolet Avatar 320 FTIR Spectrometer using the (a) thin-film method with $CHCl_3$ as solvent and (b) KBr disc method: bands are stated in cm^{-1}. NMR spectroscopy was performed on a Bruker BioSpin UltraShield NMR spectrometer at 293 ± 1 K operating at 400 MHz for ^1H, 100.62 MHz for ^{13}C and 376.46 MHz for the ^{19}F resonances. For all nine **NxxF** derivatives the ^1H spectra were acquired in $CDCl_3$ and DMSO-d_6 with ^{13}C and ^{19}F spectra run in DMSO-d_6. The NMR chemical shift values (δ) are expressed in ppm and referenced to TMS (Cl_3FC for ^{19}F NMR) and coupling constants (J) are quoted in Hz.

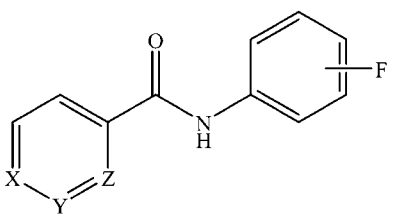

	p-fluorophenyl	*m*-fluorophenyl	*o*-fluorophenyl
para (4-pyridinoyl) (X=N, Y=C, Z=C)	**NppF**	**NpmF**	**NpoF**
meta (3-pyridinoyl) (X=C, Y=**N**, Z=C)	**NmpF**	**NmmF**	**NmoF**
ortho (2-pyridinoyl) (X=C, Y=C, Z=**N**)	**NopF**	**NomF**	**NooF**

Scheme 1 *Structures and nomenclature of the* **NxxF** *isomers.*

Ab initio molecular modeling and conformational analysis for the *gas phase* was performed at the B3LYP/6-311++G level using the Gaussian03[25] package (version E.02) for the MS Windows XP SP3 operating system running on a PC (Intel core i7-940 2.93 GHz, 8GB). The solvated form computations (PCM-SMD/B3LYP/6-311++G), conformational analyses and high accuracy energy (CBS-QB3) calculations were completed using Gaussian 09[25] for Linux/Unix operating on a Bull Novascale R422-E2 system provided by the Irish Centre for High-End Computing.

2.2 General description of the NxxF synthesis

Nucleophilic acyl substitution reactions between the fluoroanilines and pyridinoyl chlorides produced the nine *N*-(fluorophenyl)pyridinecarboxamides (**NxxF**) (x = *para*-/*meta*-/*ortho*-) (Scheme 1) in modest to high yields (20–70%). Detailed synthetic, purification procedures and all spectroscopic data are provided in the ESI† (Sections 1–3).

Condensation reactions were performed with the fluoroanilines in CH_2Cl_2: the pyridinoyl chlorides were added directly to the reaction in the presence of Et_3N. Organic washing and work-up was standard: the reaction mixture was washed with an aqueous $KHCO_3$ solution and the organic layer was dried with anhydrous $MgSO_4$. The solvent was evaporated and the **NxxF** product left for crystallization. Yields were modest to good (30–70%) in most cases with the exception of the **NoxF** isomers with lower yields of 20–30%. The product purity was mostly high (~99%), therefore crystallization and separation of the respective products from impurities was successful for most cases.

However, for the **NoxF** isomers, the accessible starting material (2-pyridinoyl chloride) was of technical grade purity containing 5-chloro-2-pyridinoyl chloride (a by-product of the 2-pyridinoyl chloride synthesis with $SOCl_2$) and solubility of the products in $CHCl_3$ was greater: re-crystallization was performed using isopropanol to give reasonably pure **NoxF** products. The physical appearance and properties (solubility and melting points) are broadly similar for all nine **NxxF** isomers and especially for the six **NpxF** and **NmxF** isomers. All **NxxF** are white, odourless, crystalline solids, soluble in $CHCl_3$, CH_2Cl_2, CH_3CN, DMSO, acetone and ethyl acetate, insoluble in water, though sparingly soluble in cold methanol and isopropanol, but with increased solubility when warmed. A substantial difference in solubility in $CHCl_3$ is evident with the **NoxF** isomers more soluble in $CHCl_3$ than the remaining six **NxxF** isomers.

2.3 Single crystal growth and X-ray diffraction methods

Single crystals of the **NxxF** compounds were grown from ethyl acetate or $CHCl_3$ by slow evaporation of the **NxxF** solutions at room temperature (294 K). Single crystal X-ray data for all nine **NxxF** isomers were collected on an Enraf-Nonius κ-CCD diffractometer at the University of Toronto at 150(1) K (except for **NppF** a non-merohedral twinned crystal [89 : 11 twin

components] at 200(1) K), θ range 2–27.5° with 100% data coverage to 25° (on θ). Data reduction procedures are standard and SORTAV was used for the absorption corrections; comprehensive details have been published elsewhere.[26,27] All structures were solved using the SHELXS97[28] direct methods program and refined by full matrix least squares calculations on F^2 with all non-hydrogen atoms having anisotropic displacement parameters (apart from disordered minor atom sites). Hydrogen atoms were treated as riding atoms using the SHELXL97 defaults (at 150 K) except for the amide N–H (isotropic refinement) using the OSCAIL software[29] with selected crystallographic and structural information in Tables 1 and 2 and the ESI† (the amide as a five atom plane). Molecular and hydrogen bonding diagrams (Fig. 1–7) were generated using PLATON.[30] All searches on the Cambridge Structural Database (CSD) were performed with the November 2009 release (version 5.31 + 3 updates).[8,31]

2.4 Computational methods

The nine **NxxF** isomers were analysed using the same methods and techniques as described previously.[12] The **NxxF** isomer optimisation and conformational analysis was performed by *ab initio* calculations (B3LYP/6-311++G) on isolated (*gas-phase*) and solvated molecules (PCM-SMD[32] solvation model with CH_2Cl_2 or H_2O) using Gaussian03/09.[25] High accuracy energy calculations (CBS-QB3)[33] were performed to obtain the ΔG of solvation and energy values are provided in the ESI† (Section 5).

Conformational analysis of the optimised **NxxF** isomers was achieved by rotation of (a) the C26–C21–C1=O1 (α dihedral, **N**-ring) and (b) the C1–N1–C11–C12 angles (β dihedral, **F**-ring) both in the *gas phase* and solvated forms to analyse and predict energetically favourable conformations.

Conformational analysis is necessary for verification of the preliminary optimised conformations as real global minima.[9] Comparisons of solid-state conformations with *ab initio* derived results were an aim, as well as calculation of rotational energy barriers for flipping the aromatic rings from one conformation to another and rationalise conformational differences > 15°. As the **NxxF** isomers have two aromatic rings connected *via* an amide linkage a total of four conformations are possible for the aromatic pyridine **N** and **F** site positions relative to the amide linkage. The rings can have the *syn* (**N**-*syn* or **F**-*syn*) or the *anti* (**N**-*anti*, **F**-*anti*) conformations (Scheme 2) and are relevant only for **NxxF** with the **N** or **F** located in *meta*- or *ortho*-sites (x = ***m*** or ***o***).

Table 1 Selected crystallographic data for the nine **NxxF** isomers[a]

NxxF	Space group	Z'	Volume/Å^3	R-factors
NppF	$P\bar{1}$	2	963.94(6)	0.051, 0.142
NpmF	Cc	1	1032.22(10)	0.042, 0.113
NpoF	Cc	1	1027.33(8)	0.051, 0.135
NmpF	$P\bar{1}$	4	1995.47(9)	0.050, 0.124
NmmF	$P2_1/n$	1	999.42(12)	0.044, 0.118
NmoF	$P2_12_12_1$	1	989.44(9)	0.049, 0.125
NopF	$P2_1/c$	1	993.10(16)	0.063, 0.166
NomF	$P2_1/n$	2	1999.17(18)	0.074, 0.223
NooF	$P2_1/n$	1	986.32(14)	0.057, 0.154

[a] Complete crystallographic, refinement and structural details for all nine **NxxF** isomers ($C_{12}H_9FN_2O$) are listed in the ESI† (Section 4).

Table 2 Relevant structural features (Å, °) in the nine **NxxF** isomers[a]

NxxF	C_6/C_5N (°)	C_6/amide	C_5N/amide	N···N/O[b]	Packing[b]
NppF*	56.74(5), 57.93(5)	29.24(7), 33.16(6)	27.63(7), 24.93(7)	3.203(2)*, 3.216(2)*	1D chains*
NpmF	65.93(10)	39.16(10)	27.39(13)	2.991(4)	2D sheets
NpoF	76.99(12)	51.39(12)	27.06(15)	2.930(4)	1D chains
NmpF	5.42(9), 0.77(10), 5.39(9), 0.74(9)	3.38(9), 1.99(9), 3.21(9), 1.56(9)	2.04(9), 2.13(9), 2.18(9), 1.82(9)	3.193(2), 3.224(2), 3.171(2), 3.254(2)	Tetrameric assembly
NmmF	50.16(5)	27.47(5)	24.00(7)	3.1146(18)	2D sheets
NmoF	22.67(14)	33.09(12)	10.75(13)	3.182(4)	1D chains
NopF	30.34(10)	27.74(11)	4.75(15)	2.679(3)	Intramolecular
NomF	4.4(2), 4.6(2)	5.5(2), 6.4(2)	2.0(2), 4.2(2)	2.675(4), 2.655(4)	Intramolecular
NooF	9.69(14)	8.67(14)	2.53(14)	2.630(3), 2.654(2)[c]	Intramolecular

[a] Full structural details are available in the ESI†. [b] The $_{amide}$N–H···$N_{pyridine}$ or N–H···O=C* interaction distances. [c] The N···F intramolecular distance.

3 Results and discussion

3.1 Comment on spectroscopic data

All spectroscopic data, including NMR and IR spectra, are provided in the ESI† (Sections 2 and 3).

The ^{1}H and ^{13}C NMR data reveal a considerable degree of similarity (as expected) and a high level of modularity (in the pyridine and fluorophenyl rings) for all nine **NxxF** isomers. Distinct trends and some salient features in the series will be discussed further. The ^{19}F NMR spectra in DMSO reveal distinct differences (δ values) with the **NxpF** series at −118 ppm and the **NxmF** triad at −112 ppm. The **NxoF** triad has both **NpoF** and **NmoF** at −121 ppm with **NooF** at −127.4 ppm highlighting the additional intramolecular hydrogen bonding effect in the **NxoF** series, but especially for **NooF** (Fig. 7).

The ^{1}H NMR δ values of the amide N–H proton lie in the range 7.91–8.15 ppm (**NpxF**) and 8.23–8.75 ppm (**NmxF**) in $CDCl_3$ and from 10.38–10.68 ppm for the six **NpxF/NmxF** isomers in DMSO-d_6 showing the increased effect of the hydrogen bonding influence (and deshielding effect) of the DMSO S=O group on the N–H proton. The distinct location of the amide proton δ values for the three **NoxF** isomers at lower-field values [10.04–10.36 ppm ($CDCl_3$) and 10.37–10.86 ppm (DMSO-d_6)] and shifted from 8 → 10 ppm in $CDCl_3$ (from **NpxF/NmxF** → **NoxF**) is due to the position and effect of the *ortho*-N atom in forming intramolecular amide N–H···N_{pyr} and intermolecular N–H···O=S interactions. However, for **NooF** the intramolecular hydrogen bonding is at a maximum with the N–H signal at 10.36 ppm ($CDCl_3$) and 10.37 ppm (DMSO-d_6) and little influenced by the DMSO solvent. Overall, the spectroscopic data for the **NoxF** triad show distinct differences amongst the nine **NxxF** isomers and highlighting the **NoxF** $_{amide}$N–H···$N_{pyridine}$ intramolecular interaction.

3.2 Crystallographic data and analysis

The principal intermolecular feature for eight of the **NxxF** crystal structures is aggregation in the crystalline state *via* $_{amide}$N–H···

$N_{pyridine}$ interactions but mostly in different crystal systems and space groups: **NppF** is the only isomer with standard N–H···O=C hydrogen bonding. Only three isomers, **NpmF**, **NmmF** and **NmoF**, crystallize with $Z' = 1$ and with no disorder: the remaining six **NxxF** crystallize with (i) $Z' > 1$ and/or (ii) C_6H_4F ring disorder and/or (iii) have a minor Cl component of impurity (derived from the original **NoxF** synthesis). Of special interest is the **NmpF** structure which forms an unusual N–H···N hydrogen bonded tetrameric assembly in the asymmetric unit, further linked by C–H···F and C–H···O=C interactions in the crystal structure.

3.2.1 NpxF series. The **NxpF** triad forms two different primary interactions as N–H···O=C in **NppF** and N–H···$N_{pyridine}$ in **NpmF**, **NpoF**.

The **NppF** isomer crystallizes in $P\bar{1}$ (no. 2) with $Z' = 2$. Data were collected at 200(1) K as a structure solution could not be obtained at 150(1) K: the results at 200(1) K with the unit cell halved revealed a non-merohedral twinned crystal with twin components of 0.89 : 0.11. PLATON[30] suggests a change to monoclinic but this is not appropriate at 200(1) K (see ESI† Section 4.1.1). Molecules A and B are non-planar (Table 2) and differ by 4° as 29.24(7)° (A) and 33.16(6)° (B) (Fig. 1) in their C_6/amide linkage angle (as five atoms). Molecules aggregate along the *a*-axis direction by $_{amide}$N–H···O=C interactions [as *C*(4) 1D chains] with long N···O distances of 3.203(2) and 3.216(2) Å in the [A···A···] and [B···B···] chains and in tandem with weak C16–H16···O1 contacts (forming $R^1_2(6)$ rings). Fluoro contacts as F···F (2.86 Å) also align in a *zigzag* chain along the *a*-axis direction. The aggregation is principally 1D and the pyridine N24A/B atoms do not participate in hydrogen bonding or even in weak contacts which is quite unusual. Obviously formation of the more common $_{amide}$N–H···$N_{pyridine}$ interactions is not favoured in **NppF** and the amide···amide hydrogen bonding forms with small additional auxiliary support from weaker C–H···O/F interactions (Fig. 1).

The **NpmF** (Fig. 2) and **NpoF** (Fig. 3) crystal structures are isomorphous in space group *Cc* (no. 9) though they differ with C_6/C_5N interplanar angles of 65.93(10)° and 76.99(12)°, respectively. Both **NpmF** and **NpoF** form short N1–H1···N24 interactions as *C*(7) *zigzag* chains with N···N distances of 2.991(4) and 2.930(4) Å, respectively. Chains are linked by longer C–H···O=C intermolecular interactions into 2D sheets parallel to the $(10\bar{1})$ plane resulting in the formation of $R^4_4(26)$ rings (Fig. 2) *via* the C15–H15···O1d interaction where symmetry code $d = -½ + x, ½ - y, -½ + z$ (*via* C13 in **NpoF**): sheets are weakly linked into a 3D structure by short C–H···π(arene) interactions. In **NpmF** the C–H···π(arene) interaction with H···Cg = 2.65 Å, C–H···Cg = 147° and C···Cg = 3.484(3) Å is not as short as that noted in the crystal structure of **Moo**.[12] Subtle differences between **NpmF** and **NpoF** are noted and especially with regard to the secondary interactions

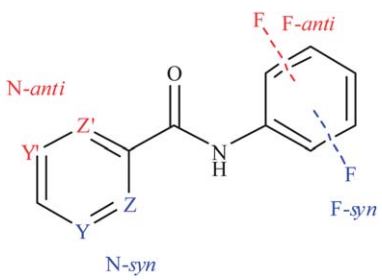

Scheme 2 Possible conformations of the **NxxF** isomers.

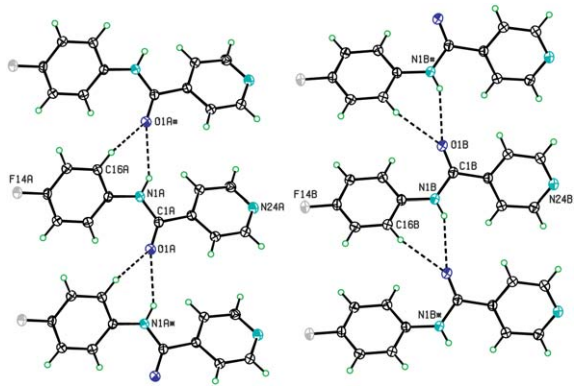

Fig. 1 The N–H···O=C and C–H···O=C interactions in **NppF** with symmetry codes # and * at positions 1 + *x*, *y*, *z* and −1 + *x*, *y*, *z*, respectively.

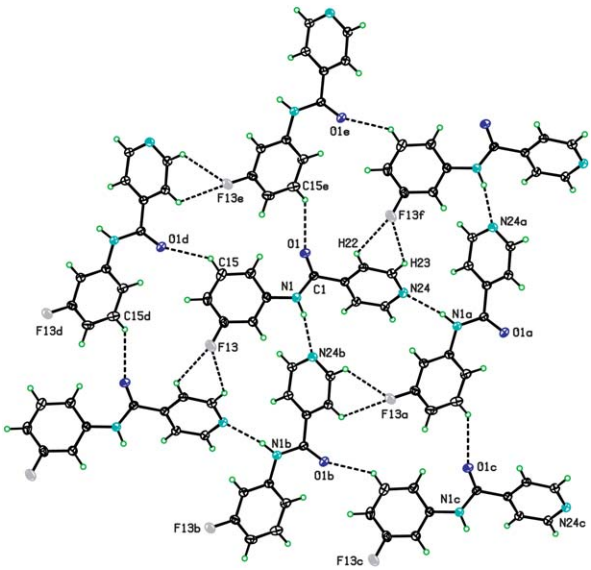

Fig. 2 The **NpmF** interactions with molecules at symmetry equivalent positions with label suffices as $a = ½ + x, -½ - y, ½ + z$; $b = -½ + x, -½ - y, -½ + z$; $c = x, y - 1, z$; $d = -½ + x, ½ - y, -½ + z$; $e = ½ + x, ½ - y, ½ + z$ and $f = 1 + x, y, 1 + z$.

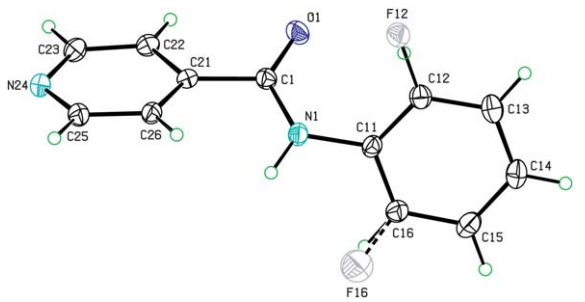

Fig. 3 The **NpoF** molecular structure with group disorder for F12 in the **F**-*anti* conformation [91.7(9)%] and F16 as **F**-*syn* [8.3(9)%].

and F atom sites. The *meta*-F13 sites [with **F**-*syn* conformations] are not disordered in **NpmF**, whereas the *ortho*-F12/F16 exhibit 0.917(9)/0.083(9) [**F**-*anti*/**F**-*syn*] conformational disorder in the **NpoF** C_6 ring involving a 180° rotation about the N1–C11 axis with H/F atoms interchanged (Fig. 3). A key reason in performing the conformational analyses is to attempt to ascertain factors (energy) which may predispose why one isomorph **NpmF** is ordered and why **NpoF** is disordered (see Section 4). Isomorphous relationships in the related **Fxx** benzamides have been reported previously,[5,11,20] while disorder is a common phenomenon in fluorobenzamides given the isosteric relationships between H and F atoms and small energy differences between the orientation of the **F**-*syn*/**F**-*anti* conformations of the C_6 aromatic rings, both in solution and the crystalline state.[5,20]

3.2.2 NmxF series. The three **NmxF** isomers aggregate *via* $_{amide}N–H\cdots N_{pyridine}$ interactions, though they differ with tetrameric assemblies in **NmpF** and as *C*(6) chains in the **NmmF** and **NmoF** isomers.

The **NmpF** isomer crystallizes as a cyclic hydrogen bonded tetrameric assembly in space group $P\bar{1}$ (no. 2) with $Z' = 4$ and in the overall shape of a '*St Brigid's*' cross (Fig. 4). In all four molecules the **Nm** ring is in the **N**-*syn* conformation. This tetrameric hydrogen bonded structure is unusual. The four molecules (A) to (D), which have approximate mirror symmetry (C_s) (with interplanar C_6/C_5N angles < 6°) differ slightly as exemplified by the four long N–H···N intermolecular hydrogen bonding distances of 3.171(2), 3.193(2), 3.224(2) and 3.254(2) Å. The cyclic tetrameric unit aggregates as an $R^4_4(24)$ ring and is augmented for each of the $N–H\cdots N_{pyridine}$ interactions by two flanking $C–H\cdots N_{pyridine}$ interactions forming $R^1_2(6)$ and $R^1_2(7)$ rings with an overall size of $R^1_3(9)$. The four flanking and longer $C16_{[A–D]}\cdots N23_{[A–D]}$ interactions are from 3.364(2) to 3.387(2) Å with the four $C22_{[A–D]}\cdots N23_{[A–D]}$ distances in the range 3.366(2) to 3.403(2) Å. The closest stacking overlap between the aromatic groups is 3.40 Å. Tetrameric units are further linked into a 3D structure by weaker C–H···F/O=C intermolecular interactions with C···F distances from 3.266(2) to 3.281(2) Å in either the *a*- and *b*-axis directions in addition to the effect of π···π stacking interactions. The C–H···O=C interactions link the tetramers along the *c*-axis direction.

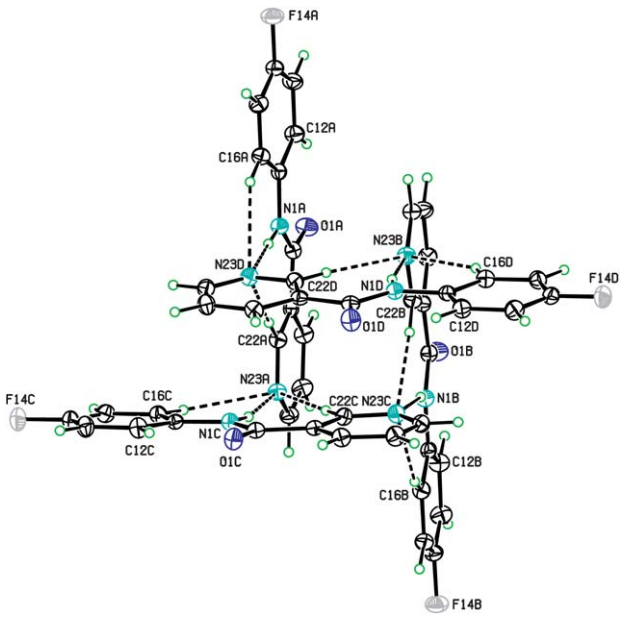

Fig. 4 The N–H···N and flanking C–H···N intermolecular interactions in the tetrameric assembly of molecules (A) to (D) in **NmpF**.

The four molecules (A) to (D) can be grouped into the A/C and B/D molecular pairs within which are close similarities. The C_6/C_5N interplanar angles are 5.42(9)°/5.39(9)° for the (A)/(C) and 0.77(10)°/0.74(9)° for the (B)/(D) pairs. There are, however, significant differences within each pair and molecules (A) and (C) have the closest fit. It is possible that a phase transition can occur at a different temperature although the **NmpF** RT (294 K) structure is similar. The unusual **NmpF** geometry (though unexpected) and assembly can be attributed to the *cis*-orientation and directional arrangement of both the N–H donor and pyridine N acceptor groups. Cyclic hydrogen bonded dimers/catemers almost certainly exist in solution but the presence of cyclic tetramers probably drives the crystallization process in a *pseudo*-macrocyclic chelation process and with the assembly held together by four N–H···N and eight C–H···N interactions.

Comparable examples of hydrogen bonded tetrameric units occur in both Ph_3COH and Ph_3GeOH where tetramers are linked by a relay of $[O–H\cdots O–H\cdots]_2$ interactions.[34,35] The crystal structure of 3-(CF_3),5-(Ph)PzH[36] [ESUJOR: CSD[8]] forms *tub-shaped* tetramers *via* N–H···N interactions as hydrogen bonded $R^4_4(12)$ rings comparable to **NmpF** in space group $P\bar{1}$ (no. 2) with $Z' = 4$; tetramers though are the least common structural motifs found amongst the *N*-unsubstituted pyrazoles.[36] The four N···N distances in ESUJOR[36] are in the range from 2.844 to 2.866 Å and the tetramer is smaller than in **NmpF**. Another series of tetrameric structures are the $[AgXL]_4$ complexes {with X = halide, L = tertiary phosphine, *e.g.* P(4-$MeC_6H_4)_3$} though the structures of $[AgXL]_4$ are very different to **NmpF**, with the *cubic vs. stella quadrangula* $[MX]_4$ cores recently discussed.[37]

The **NmmF** and **NmoF** structures are regular and both form $_{amide}N–H\cdots N_{pyridine}$ interactions as *C*(6) chains with N···N distances of 3.1146(18) Å and 3.182(4) Å, respectively. In **NmmF** the pyridyl N23 and fluoro F13 atoms are *cisoid* with respect to one another and *transoid* to the N–H group [**N**-*anti*/**F**-*anti* conformation]. The combination of the primary N–H···N interaction, C–H···O=C and two weaker interactions gives rise to a rumpled 2D sheet parallel to the $(10\bar{1})$ plane. The C_6/C_5N interplanar angle is 50.16(5)° with C_5N/amide and C_6/amide intermediate at 24.00(7)° and 27.47(5)° (Table 2). In **NmoF** this is reversed with an interplanar angle for C_6/C_5N of 22.67(14)°, whereas the C_5N/amide and C_6/amide angles are 10.75(13)° and 33.09(12)°. The pyridyl N23 and fluoro F12 are *cisoid* but are *transoid* to the C=O, in contrast to **NmmF** [**NmoF** has the **N**-*syn*/**F**-*syn* conformation]. In **NmoF**, the N–H···N primary interaction (with intramolecular C16–H16···O1, N1–H1···F12 contacts) is assisted by an intermolecular C22–H22···N23* interaction forming $R^1_2(7)$ rings with C22···N23* = 3.348(4) Å (Fig. 5); C24–H24···F12 forms an unsymmetrical $R^2_2(8)$ ring. The N–H···N interaction generates a *zigzag* 1D helical chain in the [100] direction as a stacked herringbone column (along a 2_1 axis); longer C–H···N/O/F intermolecular interactions generate a 3D network. Aromatic π···π stacking occurs with overlap of symmetry related [C11, …, C16] rings along the [100] direction [C12···C15^i = 3.307(5) Å (with $i = 1 + x, y, z$)]. For comparison the **NmoF** conformation when '*docked*' in

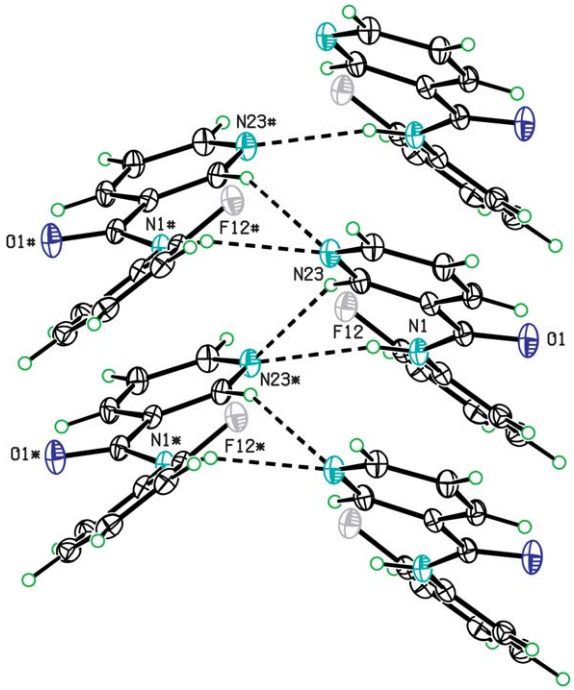

Fig. 5 The N/C–H···N hydrogen bonding in **NmoF** generates *zigzag* helical chains along the *a*-axis direction; molecules with labels # and * are located at positions ½ + *x*, −½ + *y*, −*z* and ½ + *x*, ½ + *y*, −*z*, respectively.

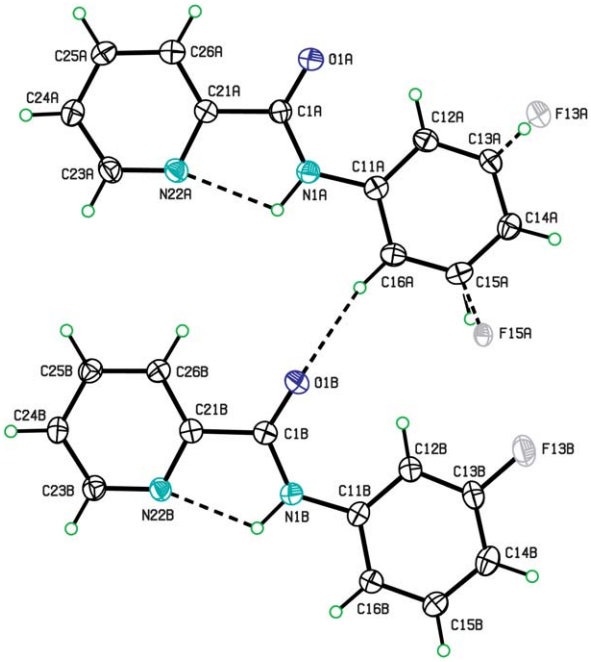

Fig. 6 The asymmetric unit of **NomF**: the minor component of disorder in molecule A (top) is at F15A.

Leishmania sirtuin (Fig. 5A in ref. 16) is similar to our **NmoF** but with the amide plane twisted by ~30°.

3.2.3 NoxF series. The primary interaction in all three **NoxF** isomers is the intramolecular N1–H1···N22 with N···N distances of 2.679(3) Å in **NopF**, 2.675(4)/2.655(4) Å in **NomF** and 2.630(3) Å in **NooF**. The **NopF** molecule has a C_6/C_5N interplanar angle of 30.34(10)°, while **NomF** and **NooF** are essentially planar molecules with approximate mirror (C_s) symmetry [C_6/C_5N angles of 4.4(2)°/4.6(2)° and 9.69(14)°], the planarity driven by the intramolecular N–H···N interaction. Disorder is observed in **NomF** and a minor Cl atom component is present as an impurity with site occupancies of 4.2(3)% and 3.2(3)% at the *meta*-C25–H25 site in **NopF** and **NooF**, respectively, and is a contaminant in the original synthesis from the acyl chloride. The minor Cl atom site component is not detected in the **NomF** structure, but there is rotational disorder in one of the C_6 rings with a minor F atom site at C15A having 6.1(5)% site occupancy ($Z' = 2$): this group disorder is similar to that described in **NpoF**. In the **Mxx** isomer grid[12] the **Mxo** triad (with an *ortho*-pyridine N atom) all aggregates using intermolecular N–H···N interactions forming hydrogen bonded dimers by centrosymmetric $R^2_2(8)$ rings. However, for the **NoxF** triad the additional C atom between the pyridyl-N and amide N–H (amide group is reversed) facilitates the additional intramolecular N–H···N_{pyr} interaction as $S(5)$ rings but mitigates against cyclic dimer formation (Fig. 6). This intramolecular interaction forces the **No** ring in all **NoxF** compounds to have the **N**-*syn* conformation.

In **NopF** the intramolecular N–H···N_{pyr} is present with an intramolecular C12–H12···O1 contact. A C16–H16···O1 interaction further links the **NopF** molecules into 1D chains along the *b*-axis direction. Weak C–H···F contacts link chains into sheets completing the structure, with molecules forming weak interactions along the *b*-axis direction parallel to the (10$\bar{2}$) plane. The related compound with CSD code, GEPQIC,[38] is the parent chloro derivative [**NopCl**] and is isomorphous with WUVYIV[39] (Br derivative as **NopBr**) but not with **NopF**.[23] The molecular overlay between the Cl/Br analogues [GEPQIC/WUVYIV] is within 0.005 Å and the C_6/C_5N interplanar rings are also close to 0°.

In **NomF** two molecules ($Z' = 2$) are present in the asymmetric unit with similar geometries and one of the molecules exhibits group disorder with a major *meta*-F13A atom site occupancy of 93.9(5)% (**N**-*syn*/**F**-*anti* conformation) and minor site at F15A (**N**-*syn*/**F**-*syn* conformation, Fig. 6). The disorder only involves 180° rotation about the N1–C11 bond and there are no other unusual artefacts of disorder/impurities in the structure. Geometric differences between the two molecules are evident, *e.g.* the C1–N1–C11–C16 angle is 177.6(3)° in molecule (A) and 172.0(3)° in (B). As in **NopF**, the **NomF** structure is remarkable for the lack of strong interactions and the strongest hydrogen bond is the intramolecular N1–H1···$N22_{pyridine}$ = 2.675(4) Å in (A), 2.655(4) Å in (B). Two intramolecular C–H···O interactions involve C12A/B at 2.845(4) Å and 2.895(4) Å. Otherwise, there are no other direction specific interactions (Fig. 6) apart from a C–H···O=C interaction (C···O = 3.362(4) Å) that links the (A) and (B) molecules within the asymmetric unit.

In **NooF** the molecular structure (Fig. 7) is essentially planar with only a small twist (<10°) of the three principal groups from co-planarity (Table 2). A minor impurity of a chloro atom is noted in a *meta* position on the pyridinyl ring. As in **NmoF**, there is molecular bending in the amide group with respect to the two terminal aromatic rings in **NooF**, with C11 at 0.087(9) Å and C21

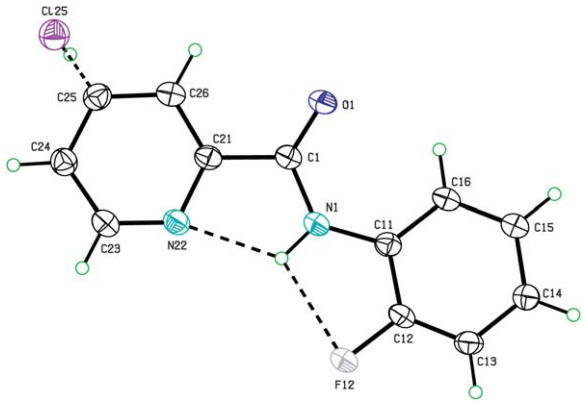

Fig. 7 The N1–H1···N22/F12 intramolecular interactions in **NooF** (with the minor Cl site depicted at C25).

at 0.033(11) Å from the O1/C1/N1 amide group plane and with C11 and C21 positioned on the same side. In **NooF** there are two distinct intramolecular interactions from the amido group as (a) N1–H1···F12 with the *ortho*-F12 [N1···F12 = 2.655(3) Å, N1–H1···F12 = 103°] and (b) N1–H1···N22 with the *ortho*-N22 [N1···N22 = 2.630(3) Å and N1–H1···N22 = 115(2)°]: C16–H16···O1 is an additional intramolecular contact (Fig. 7). These interactions facilitate the **N**-*syn*/**F**-*syn* conformation in **NooF**. Surprisingly, there are no intermolecular N1–H1···X interactions (where X = C/N/O/F) in **NooF** with the two closest N1···C atoms at 3.539(3) Å (C16 positioned at the symmetry equivalent position 1 + *x*, *y*, *z*) and at 3.577(3) Å for C23 (at *x* − 1, *y*, *z*). The closest N1···H atom contact is H23 at 3.30 Å (at −*x*, −*y*, −*z*). The lack of H bonding involving the amide N1–H1 is interesting as it is the strongest donor group in **NooF**. The dominance of the intramolecular N–H···F and N–H···N interactions with intermolecular steric packing effects prevents the close approach of suitable acceptor atoms/groups; the effect is noted in the ^{1}H NMR in DMSO-d_6. A stacking contact is present with C1···C23 (at *x* − 1, *y*, *z*) = 3.335(4) Å which manifests along the *a*-axis direction. Furthermore **NooF** is of interest as it has potential as a ligand for exploitation in coordination chemistry using a N_2F donor set.[17]

Analysis of the Cambridge Structural Database (CSD)[8,31] (version 5.31 + 3 updates) reveals six compounds reported in the literature with the same $C_{12}H_9FN_2O$ formula as the **NxxF** isomer grid. Three structures (**Fpp**, **Fmp**, **Fop**)[11] have the amide group reversed when compared to **NxxF**, however, they differ considerably in packing although the primary intermolecular interaction is $_{amide}$N–H···N$_{pyr}$.[11] Analysis of the three principal groups (2 × ring: amide) in (phenyl)benzamides on the CSD[8,31] (153 *hits* and 270 fragments, using *ortho*-ring H atoms and similar to **NxxF** for x = *p*-, *m*-) shows the three interplanar angles have mean values from 24° to 34° and similar to the interplanar angles observed in **NmoF**, though considerably greater than in the almost planar **NooF**. Where sterically bulky groups are positioned in an *ortho* position on either ring the interplanar angles increase dramatically towards orthogonality; this was observed and commented on previously in the **Mxo** series.[12]

3.2.4 Comments on molecular volumes and melting points. The symmetrical **NppF** isomer has the smallest volume per molecule [241 Å^3] at 150(1) K {in contrast to **Mpp** (Fig. 1 in ref. 12) which has the smallest with **Mop** the largest *V*/*Z* in the **Mxx** series[12]}, whereas **NpmF** [258 Å^3] and **NpoF** [257 Å^3] have the largest molecular volumes in space group *Cc*. The range of volumes for the remaining six **NxxF** molecules is narrow from 247 Å^3 for **NooF** to 250 Å^3 for **NmmF/NomF**. The average molecular volume is 250 Å^3 for all nine **NxxF** isomers as compared to 268 Å^3 for **Mxx**,[12] the difference being replacement of the F atom with CH_3 in the latter.[12]

Melting points continue to be largely ignored in solid-state chemistry[40–42] apart from listing data values and ranges. Within an isomer series with identical molecular weights and numbers of each elemental component, some general trends can be discerned and compared with literature data.[40,41] This will be of additional use in comparing expanding studies of related isomer series.[40,41] Melting point trends show the three **NoxF** compounds have the lowest melting points compared to the other six **NpxF**, **NmxF** and by ~30 to 40 °C: these six **NpxF**, **NmxF** isomers have melting points within a 23 °C range (Table 3). The highest mp is for **NpoF** (139–140 °C), the lowest is **NomF** (77.2–78 °C). The trends show as (a) the **NpxF** triad (136 °C average) > **NmxF** (124 °C) > **NoxF** (93 °C) and (b) within each of the **NxxF** triads there is a tendency for the **NxmF** to have the lowest melting points. These differences are not as dramatic as noted in the related **Mxx** series where a range of 100 °C is observed for the nine **Mxx** isomers:[12] therein, **Mmo** has the lowest melting point (78.8–80.0 °C) and similar to **NomF** (77.2–78.0 °C). The **Mxx** and **NxxF** series differ by a reversed amide bridge and substitution of a CH_3 group for an F atom on the C_6 ring with **Mxx** following the *para*-substitution > *ortho*- > *meta*-substitution melting point trend in disubstituted benzenes.[40–42] A rationalisation as why the melting point range is much greater in the **Mxx** grid in comparison to the **NxxF** series may be due to the weaker interactions. The methyl group in the **Mxx** series forms weak but favourable and cumulative secondary C–H···O/π(arene) interactions and reinforced especially in the high melting point of **Mpp** (180.2–180.8 °C).[12] In **NxxF** the effect of the F atom is smaller and weaker in supramolecular aggregation (as weaker C–H···F interactions and contacts) and does not justifiably preserve aggregation especially at the melting point event. Only in **NmpF** and **NmoF** are the C–H···F interaction distances considerably shorter (0.2 to 0.3 Å) than the contact radii. For comparisons of the **Mxo** and **NoxF** series, the *ortho*-pyridine N atom facilitates dimer formation as $R^2_2(8)$ rings in **Mxo**, but only as intramolecular $_{amide}$N–H···N$_{pyridine}$ interactions in **NoxF** and in both series only weak additional aggregation interactions are observed. These factors may explain why the **NoxF** triad has the lowest mp data in the **NxxF** series, but the **Mxo** triad as hydrogen bonded 'dimers' exhibits relatively higher average melting points.

3.3 *Ab initio* calculations

3.3.1 Structure optimisation results. The main structural aspects of the optimised **NxxF** structures are presented in Table 4. The three most important torsion angles are the C26–C21–C1═O1 angle (α) between the C_5N ring and amide group, the

Table 3 Melting point data for the **NxxF** and **Mxx**[12] derivatives

NxxF	mp/°C	Mxx[12]	mp/°C
NppF	135.0–136.5	**Mpp**	180.2–180.8
NpmF	131.2–133.6	**Mmp**	106.7[a]
NpoF	139.0–140.0	**Mop**	128.6–129.1
NmpF	131.5–133.8	**Mpm**	128.2–128.8
NmmF	121.2–122.6	**Mmm**	90.0–91.0
NmoF	116.7–118.2	**Mom**	107.5–108.5
NopF	92.0–96.0	**Mpo**	104.0–106.0
NomF	77.2–78.0	**Mmo**	78.8–80.0
NooF	105.0–108.0	**Moo**	115.0–117.1

[a] For **Mmp** the melt occurs at 106.7 °C, a partial melt at 73.8–74.5 °C.

C1–N1–C11–C12 angle (β) between the C_6 and amide group and the O1=C1–N1–C11 amide angle (δ). In general, all of the **NxxF** structures can be regarded as almost planar. The **NoxF** triad is essentially planar with no discernible differences regarding the medium (*gas phase* or solvation). The remaining six (**NpxF**, **NmxF**) isomers have torsion angles deviating from planarity. In the *gas phase* the α torsion angles of **NpxF** and **NmxF** rotate from planarity by 24.55 ± 1.67°, the δ angle by an average of 3.51 ± 0.24° and β by only 2.80 ± 0.86°. In CH_2Cl_2, the six (**NpxF**, **NmxF**) isomers have α torsion angles rotated by 29.18 ± 1.34° and β angles by an average of 3.58 ± 0.76°; the δ angle twists by 3.56 ± 0.73°. For H_2O, the **NpxF** and **NmxF** structures have α torsion angles twisted by 28.26 ± 1.07° and δ angles by 3.06 ± 0.64°. However, the β torsion angle is 11.99 ± 0.14° for **NppF** and **NmpF** but in **NpmF**, **NpoF**, **NmmF** and **NmoF** is smaller at 3.71 ± 0.58°.

Overall, optimisation of the **NxxF** isomers predicts that the three **NoxF** isomers are stabilised by the intramolecular amide N1–H1···N22 interaction (from the crystallographic and spectroscopic evidence for the relatively planar **NoxF** series, Table 2, Fig. 6 and 7). The other six **NpxF** and **NmxF** isomers distort from co-planarity mainly through pyridine ring rotation from unfavourable intramolecular H···H contacts. For the **NpxF** and **NmxF** series the only notable differences between the structures optimised in different media are the α angles (at −4.64 ± 2.28° optimised in CH_2Cl_2 and −3.71 ± 1.67° in H_2O); larger deviations occur in the β angle for **NppF** and **NmpF** optimised in water.

3.3.2 Conformational analysis. Conformational analyses in the *gas phase* establish those conformations that are favourable; Fig. 8 highlights the nine **NxxF** PES optimised in the *gas phase* including both the **N**-ring (full line) and **F**-ring (dashed line). The high modularity of all nine **NxxF** isomers is noted (as from the NMR data). Each pyridine (**N**) or fluorophenyl (**F**) group has a typical PES shape, and as each **NxxF** molecule is a combination of a **Nx** and **xF** moiety, the expected arrangement is easy to visualise with the amide link as a linker group separating both aromatic rings. For the **Np** and **pF** rings all conformations at their minima are energetically identical; for the **Nm** ring the **N**-*syn* conformation is the most stable, although the **N**-*anti* conformation is possible, but less likely. The **No** ring exists only in the **N**-*syn* conformation, while for **oF** the **F**-*syn* conformation is preferred. In **NooF** the intramolecular N1–H1···N22 interaction is augmented by the weaker N1–H1···F12 hydrogen bond (local maxima positions of both **No** and **oF** curves show that the N–H···N interaction energy is *ca.* twice the strength of the N–H···F). In comparison, the **mF** ring diagrams show that the difference between the preferred **F**-*syn* and **F**-*anti* conformations is small (0.58 kJ mol^{-1}) and both conformations are possible.

This possibility is demonstrated in two cases (a) the **NpmF** structure ($Z' = 1$) (Fig. 2) has the **F**-*syn* conformation and (b) the **NomF** structure (Fig. 6) is disordered at F15A [occupancy 6.1(5)%]. When averaged over both molecules the **mF** rings have *ca.* 3% as **F**-*syn* and 97% in the **F**-*anti* conformation.

In summary, the optimised structures (*gas phase*) typically have **N**-*syn*/**F**-*syn* conformations but the exceptions are **NxmF** where the **N**-*syn*/**F**-*anti* conformation is the most stable. Differences between the **N**-*syn*/**F**-*syn* and **N**-*syn*/**F**-*anti* conformations are small with both being plausible.

The conformational analysis results in the CH_2Cl_2 and H_2O solvents using the implicit PCM-SMD model are provided as PES scans in the ESI†. Comparisons between the *gas phase* and solvents reveal no conformation changes with all **NxpF** and **NxoF** molecules (at the stationary point) having the **N**-*syn*/**F**-*syn* conformation, while **NxmF** has the **N**-*syn*/**F**-*anti* conformations regardless of the medium. Furthermore, the patterns of maxima and minima are similar, but there are significant decreases in the rotational energy necessary for flipping rings between conformations. The implicit dielectric field in the PCM-SMD solvation model predicts a decrease of the rotational barriers with

Table 4 Torsion angles (°) of optimised **NxxF** isomers[a]

	Optimised in *gas phase*			Optimised in CH_2Cl_2			Optimised in H_2O		
	α	β	δ	α	β	δ	α	β	δ
NppF	26.67	3.72	3.20	30.35	4.04	3.27	29.47	12.09	2.43
NpmF	26.34	3.13	3.31	27.69	2.94	2.49	27.53	4.39	2.78
NpoF	23.84	1.54	3.46	30.18	3.28	3.90	27.58	3.31	2.35
NmpF	24.36	3.64	3.55	29.56	4.34	3.81	29.76	11.89	3.22
NmmF	23.81	2.68	3.74	27.28	2.57	3.23	27.29	3.15	3.79
NmoF	22.27	2.11	3.82	30.04	4.32	4.64	27.94	4.00	3.77
NopF	−0.02	0.01	−0.01	0.02	0.00	−0.02	0.01	0.01	0.00
NomF	0.00	0.00	0.01	0.06	0.02	−0.03	0.00	0.00	0.00
NooF	0.00	−0.01	0.01	0.01	−0.01	0.00	−0.02	−0.04	−0.01

[a] The angle C26–C21–C1=O1 (**N**-ring) refers to the α; C1–N1–C11–C12 angle (**F**-ring) as β and O1=C1–N1–C11 angle (amide linkage) as δ. All geometries are based on B3LYP/6-311++G optimisation with PCM-SMD solvation model.

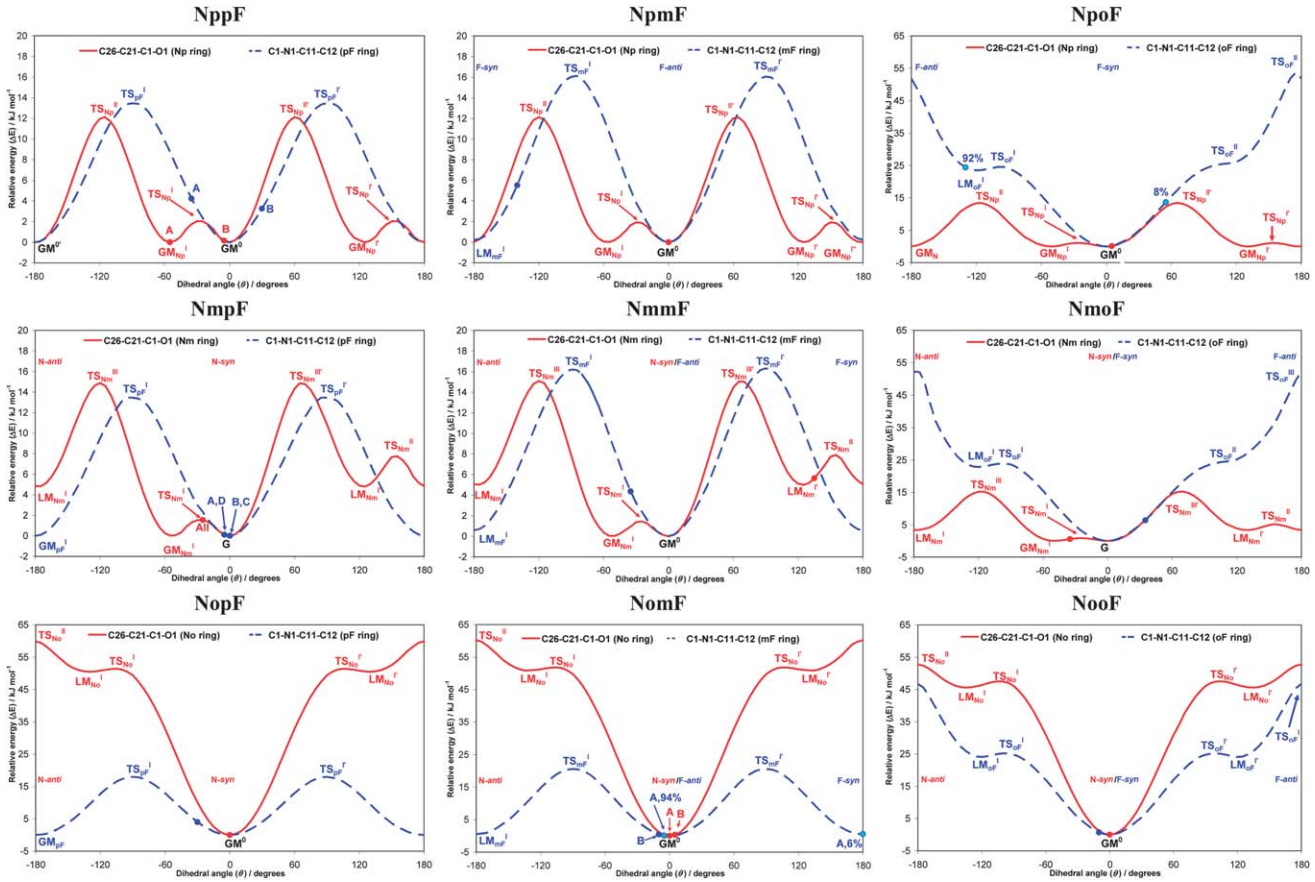

Fig. 8 The PES conformational analysis for the nine **NxxF** isomers optimised in the *gas phase*: the equivalent solid state angle is depicted by (●), with, if applicable, assigned identification letter and/or partial occurrence (%). High resolution figures and descriptions are provided in the ESI†.

potentially increasing conformational change. This model is applicable only for solvents where the **NxxF** isomers are fairly soluble. The high dielectric constant of water ($\varepsilon_r = 80$) is supposed to significantly reduce rotational barriers and disrupt the **NoxF** intramolecular interactions. However, as is evident from their insolubility in H_2O and the calculated ΔG_{solv} (Section 5, ESI†), solvation in H_2O is not favoured thermodynamically. Spectroscopic data show that a solvent with a high dielectric constant such as DMSO disrupts the intramolecular hydrogen bonds in **NoxF** and supports *ab initio* predictions and results.

4 Comparison of the NxxF isomers

The nine **NxxF** isomers derived both from calculations and crystal structures are compared by showing the differences in the corresponding torsion angles ($\Delta\theta$) as (●) for each crystal structure in each PES diagram (Fig. 8). For **NppF**, **NmpF** and **NomF** with $Z' > 1$, molecules are labelled as A, B, *etc.* and for disordered systems (**NomF**, **NpoF**) the symbol (●) has an assigned identification letter and partial occupancy (%).

In general, most solid state **NxxF** conformations correspond with their *gas phase* or solvated structures without significant torsion angle differences. Thermodynamically, formation of intermolecular bonds and contacts in the **NxxF** crystallization process brings stabilisation that is more than sufficient to overcome destabilisation from torsion angle deviations.

Differences in **NxxF** isomer conformations include (a) **NpmF** having the **F**-*syn* conformation, (b) **NmmF** with an **N**-*anti*/**F**-*anti* conformation, (c) the disordered molecule A in **NomF** where a minor F site has the **N**-*syn*/**F**-*syn* conformation and surprisingly (d) **NpoF** where the principal molecular conformation at 91.7(9)% occupancy has the **F**-ring in a metastable form in the **F**-*anti* conformation.

In almost all cases the data values for the solid-state torsion angles of the **N**-rings are on or near their calculated global minima (Fig. 8) and often with only small deviations. The exceptions include the **Nm** rings in **NmpF** and **NmmF**. For **NmpF** with $Z' = 4$ (Fig. 4) all four independent molecules are planar in the hydrogen bonded tetramer with the **Nm** ring torsion angles similar and located near TS_{Nm}^{I} which represents a relatively unstable position (*gas phase*). However, the solid-state conformation allows the *meta*-pyridine N atom to form intermolecular N1–H1···$N23_{pyr}$ hydrogen bonds augmented by two flanking C–H···N_{pyr} intermolecular interactions. Ultimately the **NmpF** supramolecular structure represents a hydrogen bonded tetramer aggregating from a series of weak but cumulatively important N/C–H···N_{pyr} interactions.

For the **NmmF** structure the **Nm** ring torsion angle has the **N**-*anti* conformation in a metastable $LM_{Nm}^{I'}$ potential well. Despite this *unusual* conformation, examination of the crystal packing shows that the **N**-*anti* conformation facilitates the 1D chain of N1–H1···N23 hydrogen bonding that is essential as the crystal structure backbone.

In contrast to the **N**-ring, the solid state **F**-ring torsion angles usually do not overlap with the corresponding *gas phase* model angle: the deviation $\Delta\theta$ is almost ± 30 to 50°, excluding the structures that are planar or close to planarity (**NmpF**, **NomF**, **NooF**) and the **NpoF** structure. The **NomF** and **NooF** are the only structures where the solid state structures correspond closely with only a slight $\Delta\theta$ deviation from the model structures.

Another phenomenon is noted in **NpmF** where the **F**-ring solid state conformation is **F**-*syn*, although the **F**-*anti* conformation is slightly thermodynamically favoured from calculations. The main backbone of the **NpmF** crystal structure is the N1–H1···N24b hydrogen bond (Fig. 2) forming *C*(7) 1D chains. As the **F**-ring adopts the **F**-*syn* conformation, the H15 atom interacts with O1 [C15···O1d = 3.202(4) Å] linking 1D chains into 2D sheets. The F13 atom forms weak contacts (as H22, H23···F13f) with neighbouring molecules, and augmenting the 2D sheets, which, *via* C25–H25···π(arene) contacts link the 2D sheets into a 3D structure. These contacts (Fig. 2) would not be possible if the F-ring adopted the **F**-*anti* conformation. A steric and repulsive clash of F13···O1d would result with the C15–H15···O1d interaction and F···H contacts negated (per molecule). Therefore, the **F**-*syn* conformation, despite its *meta*-stability in *gas phase*, is essential for the **NpmF** crystal structure assembly and stability.

The minor site with the **N**-*syn*/**F**-*syn* conformation in **NomF** (at 3% occupancy) is interesting where analysis of the **mF** ring shows that the **F**-*syn* conformation is similar to the **F**-*anti* conformation and allowing **F**-*syn* to seem statistically probable. Analysis of the **NomF** structure shows that the F atoms at their thermodynamically favoured and major site (F13A/B, **F**-*anti*) are positioned to interact with neighbouring molecules *via* weak C–H···F–C and C–F···F–C interactions with F13A···C24A = 3.339(4) Å and F13A···F13A = 2.896(3) Å. The **F**-*syn* conformation gives fewer possibilities for F···H/F/C interactions compared to the present arrangement which contributes to the overall crystal structure. Given that the difference between **F**-*syn* and **F**-*anti* is 0.58 kJ mol^{-1}, the minor **F**-*syn* conformation is presumably statistical disorder, driven by kinetic factors.

The **NpoF** structure is atypical with 91.7(9)% of the **NpoF** molecules in a thermodynamically unfavourable metastable local minimum LM_{oF}^{I} with the *ortho*-F atom at F12. The **NpoF** isomer is isomorphous with **NpmF** in space group *Cc*. A study of the crystal packing of **NpoF** shows that with the minor F16 atom site [at 8.3(9)%], positioned as **F**-*syn*, is directed near the N1–H1···N24 primary intermolecular interaction [with F16···N24 = 2.84(4) Å] and effects a measure of steric hindrance. It is possible that the **F**-*anti* (F12 site) conformation (even though it is relatively thermodynamically unstable) allows for stabilisation of the N–H···N interaction in the crystal structure. The crystal structure of **NpoF** can obviously cope with a measure of steric strain in the minor conformation (F16 atom site).

Overall, there are a few differences between the **NxxF** solid state molecular structures and the *ab initio* models and for those cases (as discussed) this arises where conformational change is essential in the promotion of favourable formation of stable intermolecular hydrogen bonds in the solid state.

5 Conclusions

In this research a 3 × 3 isomer grid of nine **NxxF** pyridinecarboxamides has been synthesised and characterised by analytical and spectroscopic methods. *Ab initio* calculations of the nine **NxxF** isomers have been performed and the energy and geometry of the optimised structures determined and analysed. The molecular and crystal structures of all nine **NxxF** isomers have been determined and compared with closely related structures on the CSD,[8,31] as well as the global minima from calculations. Eight **NxxF** structures have the $_{\text{amide}}$N–H···N$_{\text{pyridine}}$ hydrogen bond as the primary interaction with the **NppF** isomer with aggregation *via* N–H···O=C interactions. Furthermore, analysis of the disordered structures has allowed an in-depth consideration of the computational results with the crystal packing. The unusual hydrogen bonded tetramer of **NmpF** is reported with the tetrameric assembly rationalised in terms of the directional and spatial arrangements of the N–H donor and N acceptors.

The 3 × 3 isomer grid series is being expanded with key modifications to the phenyl and pyridinyl rings with a view to extending our ability to make extensive comparisons between large numbers of closely related compounds in terms of spectroscopic analysis, crystal structure analyses and computational calculations. Future research work will focus on polymorphs, solvates and salts of these isomers.

Acknowledgements

The authors thank Dublin City University and the Irish Government for postgraduate funding for Mr Pavle Močilac under the PRTLI-4 T^3 funded initiative and especially the T^3 Programme Manager Dr Neal Lemon in managing the PRTLI-4 T^3 programme. The authors thank Dr A. M. Elena and Dr J.-C. Desplat from the Irish Centre for High End Computing (ICHEC) for advice and assistance.

References

1 N. Sukumar, M. Krein and C. M. Breneman, *Curr. Opin. Drug Discovery Dev.*, 2008, **11**, 311–319.
2 R. Guha, K. Gilbert, G. Fox, M. Pierce, D. Wild and H. Yuan, *Curr. Comput.-Aided Drug Des.*, 2010, **6**, 50–67.
3 F. M. Ashcroft, *Nature*, 2006, **440**, 440–447.
4 S. Li, M. Gosling, C. T. Poll, J. Westwick and B. Cox, *Drug Discovery Today*, 2005, **10**, 129–137.
5 D. Chopra and T. N. G. Row, *CrystEngComm*, 2008, **10**, 54–67.
6 T. Gelbrich, M. B. Hursthouse and T. L. Threlfall, *Acta Crystallogr., Sect. B: Struct. Sci.*, 2007, **63**, 621–632.
7 S. M. S. V. Wardell, M. V. N. de Souza, J. L. Wardell, J. N. Low and C. Glidewell, *Acta Crystallogr., Sect. B: Struct. Sci.*, 2007, **63**, 879–895.
8 F. H. Allen, *Acta Crystallogr., Sect. B: Struct. Sci.*, 2002, **58**, 380–388.
9 C. Capacci-Daniel, S. Dehghan, V. M. Wurster, J. A. Basile, R. Hiremath, A. A. Sarjeant and J. A. Swift, *CrystEngComm*, 2008, **10**, 1875–1880.
10 G. Tuchalski, F. Emmerling, K. Groeger, A. Haensicke, T. Nagel and G. Reck, *J. Mol. Struct.*, 2006, **800**, 28–44.
11 K. Donnelly, J. F. Gallagher and A. J. Lough, *Acta Crystallogr., Sect. C: Cryst. Struct. Commun.*, 2008, **64**(6), O335–O340.
12 P. Mocilac, M. Tallon, A. J. Lough and J. F. Gallagher, *CrystEngComm*, 2010, **12**, 3080–3090.
13 G. R. Desiraju and T. Steiner, *The Weak Hydrogen Bond in Structural Chemistry and Biology*, Oxford University Press, 1999.
14 M. Nishio, M. Hirota and Y. Umezawa, *The CH/π Interaction*, Wiley, New York, 1998.
15 M. Yoshikawa, K. Motoshima, K. Fujimoto, A. Tai, H. Kakuta and K. Sasaki, *Bioorg. Med. Chem.*, 2008, **16**, 6027–6033.
16 R. U. Kadam, J. Tavares, V. M. Kiran, A. Cordeiro, A. Ouaissi and N. Roy, *Chem. Biol. Drug Des.*, 2008, **71**, 501–506.

17 S. H. van Rijt, A. J. Hebden, T. Amaresekera, R. J. Deeth, G. J. Clarkson, S. Parsons, P. C. McGowan and P. J. Sadler, *J. Med. Chem.*, 2009, **52**, 7753–7764.
18 S. I. V. Judge and C. T. Bever, *Pharmacol. Ther.*, 2006, **111**, 224–259.
19 D. T. Smith, R. Shi, R. B. Borgens, J. M. McBride, K. Jackson and S. R. Byrn, *Eur. J. Med. Chem.*, 2005, **40**, 908–917.
20 J. McMahon, F. P. Anderson, J. F. Gallagher and A. J. Lough, *Acta Crystallogr., Sect. C: Cryst. Struct. Commun.*, 2008, **64**(9), O493–O497.
21 P. M. Harrington, *Heterocycles*, 1993, **35**, 683–687.
22 J. Y. Qi, Q. Y. Yang, S. S. Chan, Z. Y. Zhou and A. S. C. Chan, *Acta Crystallogr., Sect. C: Cryst. Struct. Commun.*, 2004, **60**(5), M210–M211.
23 C. R. Wilson and O. Q. Munro, *Acta Crystallogr., Sect. C: Cryst. Struct. Commun.*, 2010, **66**(10), O513–O516.
24 W. A. Kinney, N. E. Lee, R. M. Blank, C. A. Demerson, C. S. Sarnella, N. T. Scherer, G. N. Mir, L. E. Borella, J. F. DiJoseph and C. Wells, *J. Med. Chem.*, 1990, **33**, 327–336.
25 M. J. Frisch, G. W. Trucks, H. B. Schlegel, G. E. Scuseria, M. A. Robb, J. R. Cheeseman, G. Scalmani, V. Barone, B. Mennucci, G. A. Petersson, H. Nakatsuji, M. Caricato, X. Li, H. P. Hratchian, A. F. Izmaylov, J. Bloino, G. Zheng, J. L. Sonnenberg, M. Hada, M. Ehara, K. Toyota, R. Fukuda, J. Hasegawa, M. Ishida, T. Nakajima, Y. Honda, O. Kitao, H. Nakai, T. Vreven, J. A. Montgomery, Jr, J. E. Peralta, F. Ogliaro, M. Bearpark, J. J. Heyd, E. Brothers, K. N. Kudin, V. N. Staroverov, T. Keith, R. Kobayashi, J. Normand, K. Raghavachari, A. Rendell, J. C. Burant, S. S. Iyengar, J. Tomasi, M. Cossi, N. Rega, J. M. Millam, M. Klene, J. E. Knox, J. B. Cross, V. Bakken, C. Adamo, J. Jaramillo, R. Gomperts, R. E. Stratmann, O. Yazyev, A. J. Austin, R. Cammi, C. Pomelli, J. W. Ochterski, R. L. Martin, K. Morokuma, V. G. Zakrzewski, G. A. Voth, P. Salvador, J. J. Dannenberg, S. Dapprich, A. D. Daniels, O. Farkas, J. B. Foresman, J. V. Ortiz, J. Cioslowski and D. J. Fox, *Gaussian 09, Revision B. 01*, Gaussian, Inc., Wallingford, CT, 2010.
26 *Bruker APEXII (Version 2. 0-1)*, Bruker AXS Inc., Madison, Wisconsin, USA, 2005.
27 Z. Otwinowski and W. Minor, in *Macromolecular Crystallography, Part A*, ed. J. N. Abelson, M. I. Simon, C. W. Carter and R. M. Sweet, Academic Press, Inc, New York, 1997, pp. 307–326.
28 G. M. Sheldrick, *Acta Crystallogr., Sect. A: Found. Crystallogr.*, 2008, **64**, 112–122.
29 P. McArdle, *J. Appl. Crystallogr.*, 1995, **28**, 65–65.
30 A. L. Spek, *J. Appl. Crystallogr.*, 2003, **36**, 7–13.
31 I. J. Bruno, J. C. Cole, P. R. Edgington, M. Kessler, C. F. Macrae, P. McCabe, J. Pearson and R. Taylor, *Acta Crystallogr., Sect. B: Struct. Sci.*, 2002, **58**, 389–397.
32 A. V. Marenich, C. J. Cramer and D. G. Truhlar, *J. Phys. Chem. B*, 2009, **113**, 6378–6396.
33 J. A. Montgomery, J. W. Ochterski and G. A. Petersson, *J. Chem. Phys.*, 1994, **101**, 5900–5909.
34 G. Ferguson, J. F. Gallagher, D. Murphy, T. R. Spalding, C. Glidewell and H. D. Holden, *Acta Crystallogr., Sect. C: Cryst. Struct. Commun.*, 1992, **48**, 1228–1231.
35 G. Ferguson, J. F. Gallagher, C. Glidewell, J. N. Low and S. N. Scrimgeour, *Acta Crystallogr.,Sect. C: Cryst. Struct. Commun.*, 1992, **48**, 1272–1275.
36 H. V. R. Dias and T. K. H. H. Goh, *Polyhedron*, 2004, **23**, 273–282.
37 G. J. S. Venter, A. Roodt and R. Meijboom, *Inorg. Chim. Acta*, 2009, **362**, 2475–2479.
38 Q. Zhang, S. P. Zhang and S. C. Shao, *Acta Crystallogr., Sect. E: Struct. Rep. Online*, 2006, **62**(10), O4695–O4696.
39 J. Y. Qi, Q. Y. Yang, K. H. Lam, Z. Y. Zhou and A. S. C. Chan, *Acta Crystallogr., Sect. E: Struct. Rep. Online*, 2003, **59**(3), O374–O375.
40 R. Boese, M. T. Kirchner, J. D. Dunitz, G. Filippini and A. Gavezzotti, *Helv. Chim. Acta*, 2001, **84**, 1561–1577.
41 Y. L. Slovokhotov, I. S. Neretin and J. A. K. Howard, *New J. Chem.*, 2004, **28**, 967–979.
42 A. S. Gilbert, *Thermochim. Acta*, 2007, **452**, 135–139.